

Simulation déterministe d'un MOSFET de double grille par un solveur parallèle

F. Vecil, J.M. Mantas, M.J. Cáceres, C. Sampedro, A. Godoy, F. Gámiz

Grenoble, 6 février 2014

Outline

- 1 The model
 - Introduction
 - Modelling

- 2 Numerical schemes
 - Iterative schemes for the Schrödinger-Poisson block
 - Solvers for Schrödinger and Poisson
 - Numerical methods for the BTE
 - Parallelization

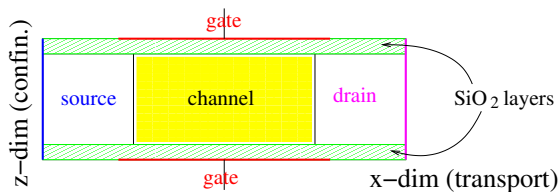
- 3 Experiments
 - Time-dependent simulations
 - Comparison to Monte-Carlo
 - Plasma oscillations (from the one-valley solver)

Outline

- 1 The model
 - Introduction
 - Modelling
- 2 Numerical schemes
 - Iterative schemes for the Schrödinger-Poisson block
 - Solvers for Schrödinger and Poisson
 - Numerical methods for the BTE
 - Parallelization
- 3 Experiments
 - Time-dependent simulations
 - Comparison to Monte-Carlo
 - Plasma oscillations (from the one-valley solver)

Geometry

The DG-MOSFET.



About the scaling

In 1971, the Intel 4004 processor had 1000 transistors, whose channel length was 10000 nm. In 1974, the Intel 8008 processor had 6-7 thousand. In 2003 the Intel Pentium IV had 50 million. Nowadays, for instance, Intel's i7-4650U has 1.3 billion transistors, whose channel is 22 nm long.

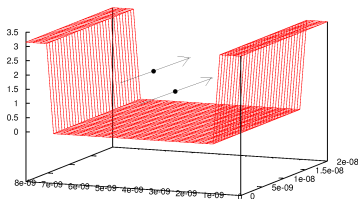
Why is it important?

Smaller MOSFETs allow for the construction of smaller devices with better performances; moreover, they allow silicon and energy saving, due to the lower voltages needed to switch on or off the transistor.

Geometry

The role of the insulating layers

Electrons are trapped inside a 3.15 V-deep well along the z -dimension. For each slice $x = \text{const}$ of the device, the energy levels are thus discrete.



The doping

This $p^+ - p - p^+$ device possesses a 10^{26}m^{-3} doping at the source and the drain, 10^{18}m^{-3} at the channel. The doping attempts to control the electrical properties (conductivity) of the device.

The gates

The gates are metallic contacts. The potential applied at them has the role of a “tap” that allows or prevents the flow of current across the device.

Outline

- 1 The model
 - Introduction
 - **Modelling**
- 2 Numerical schemes
 - Iterative schemes for the Schrödinger-Poisson block
 - Solvers for Schrödinger and Poisson
 - Numerical methods for the BTE
 - Parallelization
- 3 Experiments
 - Time-dependent simulations
 - Comparison to Monte-Carlo
 - Plasma oscillations (from the one-valley solver)

The confinement

Dimensional coupling

Electrons are **particles** along the x -dimension, **waves** along the z -dimension.

Description of the confinement

A set of 1D Schrödinger eigenvalue problems describe the electrons along z .

$$-\frac{\hbar^2}{2} \frac{d}{dz} \left[\frac{1}{m_{z,\nu}} \frac{d\psi_{\nu,p}[V]}{dz} \right] - q(V + V_c) \psi_{\nu,p}[V] = \epsilon_{\nu,p}[V] \psi_{\nu,p}[V]$$

Subbands and wave functions

The eigenvalues $\{\epsilon_{\nu,p}\}_{(\nu,p) \in \{1,2,3\} \times \mathbb{Z}_{>0}}$ represent the energy levels, called *subbands* in physics.

The eigenfunctions $\{\psi_{\nu,p}(\cdot)\}_{(\nu,p) \in \{1,2,3\} \times \mathbb{Z}_{>0}}$ are called *wave functions* in physics.

Electron population

The subbands decompose the electron population of the ν^{th} **valley** into independent populations. The densities are indexed on the pair (ν, p) .

The confinement

Dimensional coupling

Electrons are **particles** along the x -dimension, **waves** along the z -dimension.

Description of the confinement

A set of 1D Schrödinger eigenvalue problems describe the electrons along z .

$$-\frac{\hbar^2}{2} \frac{d}{dz} \left[\frac{1}{m_{z,\nu}} \frac{d\psi_{\nu,p}[V]}{dz} \right] - q(V + V_c) \psi_{\nu,p}[V] = \epsilon_{\nu,p}[V] \psi_{\nu,p}[V]$$

Subbands and wave functions

The eigenvalues $\{\epsilon_{\nu,p}\}_{(\nu,p) \in \{1,2,3\} \times \mathbb{Z}_{>0}}$ represent the energy levels, called *subbands* in physics.

The eigenfunctions $\{\psi_{\nu,p}(\cdot)\}_{(\nu,p) \in \{1,2,3\} \times \mathbb{Z}_{>0}}$ are called *wave functions* in physics.

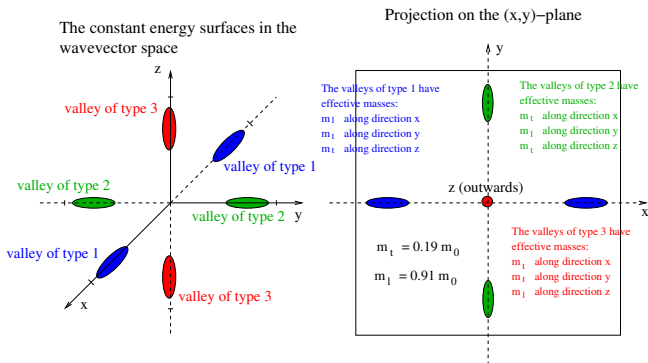
Electron population

The subbands decompose the electron population of the ν^{th} **valley** into independent populations. The densities are indexed on the pair (ν, p) .

Band structure

The three valleys

The Si band structure presents six minima in the first Brillouin zone:



The axes of the ellipsoids are disposed along the x , y and z axes of the reciprocal lattice. The three minima have the same value, therefore there is no gap.

Band structure

Non-parabolicity

The band structure around the three minima can be expanded following the Kane non-parabolic approximation (ν indexes the valley):

$$\epsilon_{\nu}^{\text{kin}}(k_x, k_y) = \frac{\hbar^2}{1 + \sqrt{1 + 2\tilde{\alpha}_{\nu}\hbar^2 \left(\frac{k_x^2}{m_e m_{x,\nu}} + \frac{k_y^2}{m_e m_{y,\nu}} \right)}} \left(\frac{k_x^2}{m_e m_{x,\nu}} + \frac{k_y^2}{m_e m_{y,\nu}} \right),$$

where $m_{x,\nu}$ and $m_{y,\nu}$ are the effective masses along the unconfined dimensions and the $\tilde{\alpha}_{\nu}$ are the Kane dispersion factors.

z -direction

The band structure does not depend on z as the carriers are not free to move along that direction.

Electron population

The total amount of carriers is split into independent populations, one for each valley. We shall index them $\nu = 1, 2, 3$.

The unconfined dimension

BTE

The Boltzmann Transport Equation (one for each pair (ν, p)) reads

$$\frac{\partial f_{\nu,p}}{\partial t} + \overbrace{\frac{1}{\hbar} \frac{\partial \epsilon_{\nu}^{\text{kin}}}{\partial k_x} \frac{\partial f_{\nu,p}}{\partial x}}^{\text{free motion}} - \overbrace{\frac{1}{\hbar} \frac{\partial \epsilon_{\nu,p}}{\partial x} \frac{\partial f_{\nu,p}}{\partial k_x}}^{\text{force field}} = \overbrace{\mathcal{Q}_{\nu,p}[f]}^{\text{scatterings}},$$

$$f_{\nu,p}(t=0, x, \mathbf{k}) = \underbrace{\varrho_{\nu,p}^{\text{eq}}(x)}_{\text{equil. dens.}} \underbrace{M_{\nu}(\mathbf{k})}_{\text{Maxw.}}$$

The collision operator

Electrons are scattered by the vibration of the crystal lattice, described as phonons:

$$\mathcal{Q}_{\nu,p}[f] = \sum_s \sum_{\nu', p'} \int_{\mathbb{R}^2} [S_{(\nu', p', \mathbf{k}') \rightarrow (\nu, p, \mathbf{k})}^s f_{\nu', p'}(\mathbf{k}') - S_{(\nu, p, \mathbf{k}) \rightarrow (\nu', p', \mathbf{k}')}^s f_{\nu, p}(\mathbf{k})] d\mathbf{k}'.$$

Remark. In an unconfined setting, we would rather have something like

$$\mathcal{Q}[f] = \sum_s \int_{\mathbb{R}^3} [S_{\mathbf{k}' \rightarrow \mathbf{k}}^s f(\mathbf{k}') - S_{\mathbf{k} \rightarrow \mathbf{k}'}^s f(\mathbf{k})] d\mathbf{k}'.$$

Eigenstates, mixed states and classical states.

The classical states are the magnitudes which only depend on the unconfined dimension x , while mixed states depend on both x and z .

Eigenstates

The subbands and the wave functions $\{\epsilon_{\nu,p}(x), \psi_{\nu,p}(x, \cdot)\}_{(\nu,p) \in \{1,2,3\} \times \mathbb{Z}_{>0}}$ are eigenstates; they depend on x only as a parameter.

Classical states

The pdf's $\{f_{\nu,p}(t, x, \mathbf{k})\}_{\nu,p}$ are classical states, therefore the surface density

$$\varrho(t, x) = 2 \sum_{\nu=1}^3 \sum_{p=1}^{\infty} \int_{\mathbb{R}^2} f_{\nu,p}(t, x, \mathbf{k}) \, d\mathbf{k}$$

is a classical state too, and in general most of the macroscopic magnitudes.

Mixed states

The electrostatic potential $V(x, z)$ and the volume density

$$N(t, x, z) = 2 \sum_{\nu=1}^3 \sum_{p=1}^{\infty} \int_{\mathbb{R}^2} f_{\nu,p}(t, x, \mathbf{k}) \, d\mathbf{k} |\psi_{\nu,p}(t, x, z)|^2$$

are mixed states.

The model

BTE

The Boltzmann Transport Equation (one for each pair (ν, p)) reads

$$\frac{\partial f_{\nu,p}}{\partial t} + \frac{1}{\hbar} \frac{\partial \epsilon_{\nu}^{\text{kin}}}{\partial k_x} \frac{\partial f_{\nu,p}}{\partial x} - \frac{1}{\hbar} \frac{\partial \epsilon_{\nu,p}}{\partial x} \frac{\partial f_{\nu,p}}{\partial k_x} = \mathcal{Q}_{\nu,p}[f].$$

Schrödinger-Poisson block

$$-\frac{\hbar^2}{2} \frac{d}{dz} \left[\frac{1}{m_{z,\nu}} \frac{d\psi_{\nu,p}[V]}{dz} \right] - q(V + V_c) \psi_{\nu,p}[V] = \epsilon_{\nu,p}[V] \psi_{\nu,p}[V]$$

$$-\text{div}_{x,z} [\epsilon_R \nabla_{x,z} V] = -\frac{q}{\epsilon_0} (N[V] - N_D), \quad N[V] = 2 \sum_{\nu,p} \varrho_{\nu,p} |\psi_{\nu,p}[V]|^2$$

These equations cannot be decoupled because we need the **eigenfunctions** to compute the potential, and we need the potential to compute the eigenfunctions.

The model

BTE

The Boltzmann Transport Equation (one for each pair (ν, p)) reads

$$\frac{\partial f_{\nu,p}}{\partial t} + \frac{1}{\hbar} \frac{\partial \epsilon_{\nu}^{\text{kin}}}{\partial k_x} \frac{\partial f_{\nu,p}}{\partial x} - \frac{1}{\hbar} \frac{\partial \epsilon_{\nu,p}}{\partial x} \frac{\partial f_{\nu,p}}{\partial k_x} = \mathcal{Q}_{\nu,p}[f].$$

Schrödinger-Poisson block

$$-\frac{\hbar^2}{2} \frac{d}{dz} \left[\frac{1}{m_{z,\nu}} \frac{d\psi_{\nu,p}[\mathbf{V}]}{dz} \right] - q(V + V_c) \psi_{\nu,p}[\mathbf{V}] = \epsilon_{\nu,p}[\mathbf{V}] \psi_{\nu,p}[\mathbf{V}]$$

$$-\text{div}_{x,z} [\epsilon_R \nabla_{x,z} V] = -\frac{q}{\epsilon_0} (N[\mathbf{V}] - N_D), \quad N[\mathbf{V}] = 2 \sum_{\nu,p} \varrho_{\nu,p} |\psi_{\nu,p}[\mathbf{V}]|^2$$

These equations cannot be decoupled because we need the **eigenfunctions** to compute the potential, and we need the potential to compute the eigenfunctions.

The model

The collision operator

The collision operator takes into account the phonon scattering mechanism. It reads

$$\mathcal{Q}_{\nu,p}[f] = \sum_s \sum_{\nu',p'} \int_{\mathbb{R}^2} [S_{(\nu',p',k') \rightarrow (\nu,p,k)}^s f_{\nu',p'}(k') - S_{(\nu,p,k) \rightarrow (\nu',p',k')}^s f_{\nu,p}(k)] dk'.$$

Structure of the S^s

The missing dimension of the wave-vector $k \in \mathbb{R}^2$, instead of $k \in \mathbb{R}^3$, is replaced by an overlap integral $W_{(\nu,p) \leftrightarrow (\nu',p')}$:

$$S_{(\nu,p,k) \rightarrow (\nu',p',k')}^s = C_{\nu \rightarrow \nu'} \frac{1}{W_{(\nu,p) \leftrightarrow (\nu',p')}} \delta(\epsilon_{\nu',p'}^{\text{tot}}(k') - \epsilon_{\nu,p}^{\text{tot}}(k) \pm \text{some energy})$$

$$\frac{1}{W_{(\nu,p) \leftrightarrow (\nu',p')}} = \int_0^{L_z} |\psi_{\nu,p}|^2 |\psi_{\nu',p'}|^2 dz, \quad [W] = m.$$

The model

The collision operator

The collision operator takes into account the phonon scattering mechanism. It reads

$$\mathcal{Q}_{\nu,p}[f] = \sum_s \sum_{\nu',p'} \int_{\mathbb{R}^2} [S_{(\nu',p',k') \rightarrow (\nu,p,k)}^s f_{\nu',p'}(k') - S_{(\nu,p,k) \rightarrow (\nu',p',k')}^s f_{\nu,p}(k)] dk'.$$

Structure of the S^s

The missing dimension of the wave-vector $\mathbf{k} \in \mathbb{R}^2$, instead of $\mathbf{k} \in \mathbb{R}^3$, is replaced by an overlap integral $W_{(\nu,p) \leftrightarrow (\nu',p')}$:

$$S_{(\nu,p,k) \rightarrow (\nu',p',k')}^s = C_{\nu \rightarrow \nu'} \frac{1}{W_{(\nu,p) \leftrightarrow (\nu',p')}} \delta(\epsilon_{\nu',p'}^{\text{tot}}(k') - \epsilon_{\nu,p}^{\text{tot}}(k) \pm \text{some energy})$$

$$\frac{1}{W_{(\nu,p) \leftrightarrow (\nu',p')}} = \int_0^{L_z} |\psi_{\nu,p}|^2 |\psi_{\nu',p'}|^2 dz, \quad [W] = m.$$

Initial condition

Strategy

We want to initialize the system under the following constraints:

- Fulfill electrical neutrality at the source contact:

$$\int_0^{L_z} N_D(0, z) dz = \int_0^{L_z} N(0, z) dz.$$

- Have a thermodynamical equilibrium for the system, i.e. a distribution which is a zero for both the BTE and the scattering operator.
- (Cope with the former work of Carlos and Andrés.)

Step 1: the potential at the metallic contacts

Solve Schrödinger-Poisson for the following density:

$$N[V] = \frac{2}{\pi} \frac{m_e \kappa_B T_L}{\hbar^2} \sum_{\nu, p} \sqrt{m_{x, \nu} m_{y, \nu}} \ln \left(1 + e^{-\frac{\epsilon_{\nu, p}[V](x) - \epsilon_F}{\kappa_B T_L}} \right) |\psi_{\nu, p}[V](x, z)|^2$$

with homogeneous Neumann boundary conditions everywhere except at gate contacts. We retain the profile of V at the contacts: $V_b(z) = V(0, z)$.

Initial condition

Strategy

We want to initialize the system under the following constraints:

- Fulfill electrical neutrality at the source contact:

$$\int_0^{L_z} N_D(0, z) dz = \int_0^{L_z} N(0, z) dz.$$

- Have a thermodynamical equilibrium for the system, i.e. a distribution which is a zero for both the BTE and the scattering operator.
- (Cope with the former work of Carlos and Andrés.)

Step 1: the potential at the metallic contacts

Solve Schrödinger-Poisson for the following density:

$$N[V] = \frac{2}{\pi} \frac{m_e \kappa_B T_L}{\hbar^2} \sum_{\nu, p} \sqrt{m_{x, \nu} m_{y, \nu}} \ln \left(1 + e^{-\frac{\epsilon_{\nu, p}[V](x) - \epsilon_F}{\kappa_B T_L}} \right) |\psi_{\nu, p}[V](x, z)|^2$$

with homogeneous Neumann boundary conditions everywhere except at gate contacts. We retain the profile of V at the contacts: $V_b(z) = V(0, z)$.

Outline

- 1 The model
 - Introduction
 - Modelling
- 2 Numerical schemes
 - **Iterative schemes for the Schrödinger-Poisson block**
 - Solvers for Schrödinger and Poisson
 - Numerical methods for the BTE
 - Parallelization
- 3 Experiments
 - Time-dependent simulations
 - Comparison to Monte-Carlo
 - Plasma oscillations (from the one-valley solver)

The Newton scheme

The functional

Solving the Schrödinger-Poisson block

$$\begin{aligned}
 -\frac{\hbar^2}{2} \frac{d}{dz} \left[\frac{1}{m_{z,\nu}} \frac{d\psi_{\nu,p}[V]}{dz} \right] - q(V + V_c) \psi_{\nu,p}[V] &= \epsilon_{\nu,p}[V] \psi_{\nu,p}[V] \\
 -\operatorname{div} [\epsilon_R \nabla V] &= -\frac{q}{\epsilon_0} (N[V] - N_D)
 \end{aligned}$$

is equivalent to seeking for the zero, under the constraints of the Schrödinger equation, of the functional $P[V]$

$$P[V] = -\operatorname{div} (\epsilon_R \nabla V) + \frac{q}{\epsilon_0} (N[V] - N_D),$$

The scheme

which is achieved by means of a Newton-Raphson iterative scheme

$$dP(V^{\text{old}}, V^{\text{new}} - V^{\text{old}}) = -P[V^{\text{old}}], \quad d = \text{Gâteaux-derivative.}$$

The Newton scheme

The functional

Solving the Schrödinger-Poisson block

$$\begin{aligned}
 -\frac{\hbar^2}{2} \frac{d}{dz} \left[\frac{1}{m_{z,\nu}} \frac{d\psi_{\nu,p}[V]}{dz} \right] - q(V + V_c) \psi_{\nu,p}[V] &= \epsilon_{\nu,p}[V] \psi_{\nu,p}[V] \\
 -\operatorname{div} [\epsilon_R \nabla V] &= -\frac{q}{\epsilon_0} (N[V] - N_D)
 \end{aligned}$$

is equivalent to seeking for the zero, under the constraints of the Schrödinger equation, of the functional $P[V]$

$$P[V] = -\operatorname{div} (\epsilon_R \nabla V) + \frac{q}{\epsilon_0} (N[V] - N_D),$$

The scheme

which is achieved by means of a Newton-Raphson iterative scheme

$$dP(V^{\text{old}}, V^{\text{new}} - V^{\text{old}}) = -P[V^{\text{old}}], \quad d = \text{Gâteaux-derivative.}$$

The iterations

Derivatives

The Gâteaux-derivatives of the eigenproperties are needed:

$$\begin{aligned} d\epsilon_{\nu,p}(V, U) &= -q \int U(\zeta) |\psi_{\nu,p}[V](\zeta)|^2 d\zeta \\ d\psi_{\nu,p}(V, U) &= -q \sum_{p' \neq p} \frac{\int U(\zeta) \psi_{\nu,p}[V](\zeta) \psi_{\nu,p'}[V](\zeta) d\zeta}{\epsilon_{\nu,p}[V] - \epsilon_{\nu,p'}[V]} \psi_{\nu,p'}[V](z). \end{aligned}$$

Iterations

After computing the Gâteaux-derivative of the density and developping calculations, we are led to a Poisson-like equation

$$\begin{aligned} & -\operatorname{div}(\epsilon_R \nabla V^{\text{new}}) + \int_0^{L_z} \mathcal{A}[V^{\text{old}}](z, \zeta) V^{\text{new}}(\zeta) d\zeta \\ &= -\frac{q}{\epsilon_0} (N[V^{\text{old}}] - N_D) + \int_0^{L_z} \mathcal{A}[V^{\text{old}}](z, \zeta) V^{\text{old}}(\zeta) d\zeta, \end{aligned}$$

where $\mathcal{A}[V]$ is essentially the Gâteaux-derivative of the density $N[V]$.

The iterations

Derivatives

The Gâteaux-derivatives of the eigenproperties are needed:

$$\begin{aligned} d\epsilon_{\nu,p}(V, U) &= -q \int U(\zeta) |\psi_{\nu,p}[V](\zeta)|^2 d\zeta \\ d\psi_{\nu,p}(V, U) &= -q \sum_{p' \neq p} \frac{\int U(\zeta) \psi_{\nu,p}[V](\zeta) \psi_{\nu,p'}[V](\zeta) d\zeta}{\epsilon_{\nu,p}[V] - \epsilon_{\nu,p'}[V]} \psi_{\nu,p'}[V](z). \end{aligned}$$

Iterations

After computing the Gâteaux-derivative of the density and developping calculations, we are led to a Poisson-like equation

$$\begin{aligned} & -\operatorname{div}(\epsilon_R \nabla V^{\text{new}}) + \int_0^{L_z} \mathcal{A}[V^{\text{old}}](z, \zeta) V^{\text{new}}(\zeta) d\zeta \\ &= -\frac{q}{\epsilon_0} (N[V^{\text{old}}] - N_D) + \int_0^{L_z} \mathcal{A}[V^{\text{old}}](z, \zeta) V^{\text{old}}(\zeta) d\zeta, \end{aligned}$$

where $\mathcal{A}[V]$ is essentially the Gâteaux-derivative of the density $N[V]$.

Comparison Newton-Raphson vs. Gummel

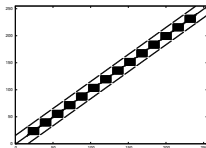
Gummel

$$-\operatorname{div}(\varepsilon_R \nabla V^{\text{new}}) + \frac{q^2}{\varepsilon_0 k_B T_L} N V^{\text{new}} = -\frac{q}{\varepsilon_0} (N - N_D) + \frac{q^2}{\varepsilon_0 k_B T_L} N V^{\text{old}}$$

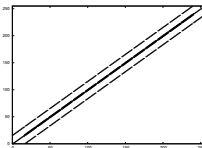
Newton-Raphson

$$-\operatorname{div}(\varepsilon_R \nabla V^{\text{new}}) + \int_0^{L_z} \mathcal{A}(z, \zeta) V^{\text{new}}(\zeta) d\zeta = -\frac{q}{\varepsilon_0} (N - N_D) + \int_0^{L_z} \mathcal{A}(z, \zeta) V^{\text{old}}(\zeta) d\zeta$$

Comparison



(a) Newton-Raphson



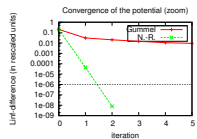
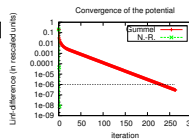
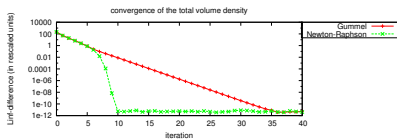
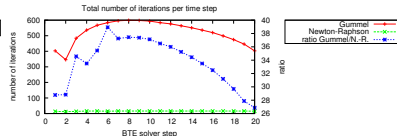
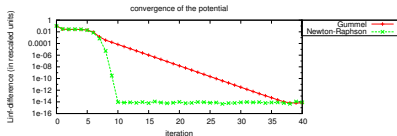
(b) Gummel



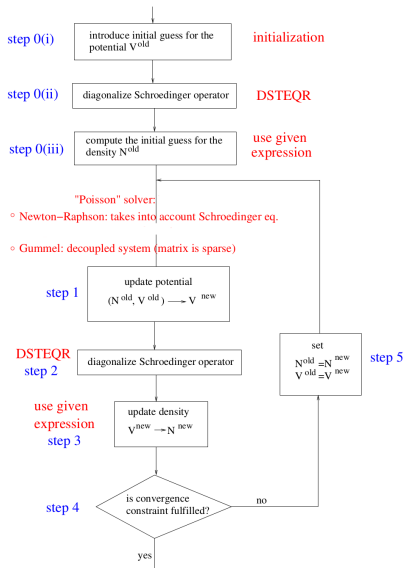
Iterative schemes for the Schrödinger-Poisson block

Comparison Newton-Raphson vs. Gummel

Gummel vs NR



Framework



Outline

- 1 The model
 - Introduction
 - Modelling
- 2 Numerical schemes
 - Iterative schemes for the Schrödinger-Poisson block
 - **Solvers for Schrödinger and Poisson**
 - Numerical methods for the BTE
 - Parallelization
- 3 Experiments
 - Time-dependent simulations
 - Comparison to Monte-Carlo
 - Plasma oscillations (from the one-valley solver)

Numerical methods

We need to solve the Schrödinger eigenvalue problem and Poisson equations.

The Schrödinger equation

Equation

$$-\frac{\hbar^2}{2} \frac{d}{dz} \left[\frac{1}{m_{z,\nu}} \frac{d\psi_{\nu,p}}{dz} \right] - q(V + V_c) \psi_{\nu,p} = \epsilon_{\nu,p} \psi_{\nu,p}$$

is discretized by alternate finite differences for the derivatives then the symmetric matrix is diagonalized by a LAPACK routine called DSTEQR.

The Poisson equation

We need to solve equations like

$$-\text{div} [\epsilon_R \nabla V] + \int_0^{L_z} \mathcal{A}(z, \zeta) V(\zeta) d\zeta = \text{rhs}$$

The derivatives are discretized by finite differences in alternate directions, the integral is computed via trapezoid rule and the banded linear system is solved by means of Library of Iterative Solvers “-i idrs -p iluc -tol 1.0e-12”.

Numerical methods

We need to solve the Schrödinger eigenvalue problem and Poisson equations.

The Schrödinger equation

Equation

$$-\frac{\hbar^2}{2} \frac{d}{dz} \left[\frac{1}{m_{z,\nu}} \frac{d\psi_{\nu,p}}{dz} \right] - q(V + V_c) \psi_{\nu,p} = \epsilon_{\nu,p} \psi_{\nu,p}$$

is discretized by alternate finite differences for the derivatives then the symmetric matrix is diagonalized by a LAPACK routine called DSTEQR.

The Poisson equation

We need to solve equations like

$$-\text{div} [\epsilon_R \nabla V] + \int_0^{L_z} \mathcal{A}(z, \zeta) V(\zeta) d\zeta = \text{rhs}$$

The derivatives are discretized by finite differences in alternate directions, the integral is computed via trapezoid rule and the banded linear system is solved by means of Library of Iterative Solvers “-i idrs -p iluc -tol 1.0e-12”.

Numerical methods

We need to solve the Schrödinger eigenvalue problem and Poisson equations.

The Schrödinger equation

Equation

$$-\frac{\hbar^2}{2} \frac{d}{dz} \left[\frac{1}{m_{z,\nu}} \frac{d\psi_{\nu,p}}{dz} \right] - q(V + V_c) \psi_{\nu,p} = \epsilon_{\nu,p} \psi_{\nu,p}$$

is discretized by alternate finite differences for the derivatives then the symmetric matrix is diagonalized by a LAPACK routine called DSTEQR.

The Poisson equation

We need to solve equations like

$$-\text{div} [\epsilon_R \nabla V] + \int_0^{L_z} \mathcal{A}(z, \zeta) V(\zeta) d\zeta = \text{rhs}$$

The derivatives are discretized by finite differences in alternate directions, the integral is computed via trapezoid rule and the banded linear system is solved by means of Library of Iterative Solvers “*-i idrs -p iluc -tol 1.0e-12*”.

Outline

- 1 The model
 - Introduction
 - Modelling
- 2 Numerical schemes
 - Iterative schemes for the Schrödinger-Poisson block
 - Solvers for Schrödinger and Poisson
 - **Numerical methods for the BTE**
 - Parallelization
- 3 Experiments
 - Time-dependent simulations
 - Comparison to Monte-Carlo
 - Plasma oscillations (from the one-valley solver)

Adimensionalization of the wave-vector space

The wave-vector space is adimensionalized by a change of variables into ellipsoidal variables, in order to better integrate the scattering operator and to have a simple expression for the kinetic energy and related magnitudes.

Ellipsoidal coordinated

The wave-vector for the ν^{th} valley reads:

$$(\tilde{k}_x, \tilde{k}_y) = \frac{\sqrt{m_e \kappa_B T_L}}{\hbar} \sqrt{2w(1 + \alpha_\nu w)} (\sqrt{m_{x,\nu}} \cos(\phi), \sqrt{m_{y,\nu}} \sin(\phi)).$$

The Jacobian

The magnitude $s_\nu(w)$ represents the dimensionless Jacobian of the change of variables in the wave-vector space:

$$s_\nu(w) = \left| \det \frac{\partial (k_x, k_y)}{\partial (w, \phi)} \right| = \sqrt{m_{x,\nu} m_{y,\nu}} (1 + 2\alpha_\nu w).$$

Adimensionalization of the wave-vector space

The wave-vector space is adimensionalized by a change of variables into ellipsoidal variables, in order to better integrate the scattering operator and to have a simple expression for the kinetic energy and related magnitudes.

Ellipsoidal coordinated

The wave-vector for the ν^{th} valley reads:

$$(\tilde{k}_x, \tilde{k}_y) = \frac{\sqrt{m_e \kappa_B T_L}}{\hbar} \sqrt{2w(1 + \alpha_\nu w)} (\sqrt{m_{x,\nu}} \cos(\phi), \sqrt{m_{y,\nu}} \sin(\phi)) .$$

The Jacobian

The magnitude $s_\nu(w)$ represents the dimensionless Jacobian of the change of variables in the wave-vector space:

$$s_\nu(w) = \left| \det \frac{\partial (k_x, k_y)}{\partial (w, \phi)} \right| = \sqrt{m_{x,\nu} m_{y,\nu}} (1 + 2\alpha_\nu w) .$$

BTE in ellipsoidal coordinates

Let the flux coefficients

$$\begin{aligned}
 a_{\nu}^1(w, \phi) &= \frac{\sqrt{2w(1 + \alpha_{\nu}w)} \cos(\phi)}{\sqrt{m_{x,\nu}}} \frac{1}{1 + 2\alpha_{\nu}w} \\
 a_{\nu,p}^2(x, w, \phi) &= -\frac{\partial \epsilon_{\nu,p}}{\partial x} \frac{1}{1 + 2\alpha_{\nu}w} \frac{\sqrt{2w(1 + \alpha_{\nu}w)} \cos(\phi)}{\sqrt{m_{x,\nu}}} \\
 a_{\nu,p}^3(x, w, \phi) &= \frac{\partial \epsilon_{\nu,p}}{\partial x} \frac{\sin(\phi)}{\sqrt{m_{x,\nu}} \sqrt{2w(1 + \alpha_{\nu}w)}}.
 \end{aligned}$$

Conservation-law form

$$\frac{\partial \Phi_{\nu,p}}{\partial t} + \frac{\partial}{\partial x} [a_{\nu}^1 \Phi_{\nu,p}] + \frac{\partial}{\partial w} [a_{\nu,p}^2 \Phi_{\nu,p}] + \frac{\partial}{\partial \phi} [a_{\nu,p}^3 \Phi_{\nu,p}] = \mathcal{Q}_{\nu,p}[\Phi]s(w)$$

BTE in ellipsoidal coordinates

Let the flux coefficients

$$a_{\nu}^1(w, \phi) = \frac{\sqrt{2w(1 + \alpha_{\nu}w)} \cos(\phi)}{\sqrt{m_{x,\nu}}} \frac{1}{1 + 2\alpha_{\nu}w}$$

$$a_{\nu,p}^2(x, w, \phi) = -\frac{\partial \epsilon_{\nu,p}}{\partial x} \frac{1}{1 + 2\alpha_{\nu}w} \frac{\sqrt{2w(1 + \alpha_{\nu}w)} \cos(\phi)}{\sqrt{m_{x,\nu}}}$$

$$a_{\nu,p}^3(x, w, \phi) = \frac{\partial \epsilon_{\nu,p}}{\partial x} \frac{\sin(\phi)}{\sqrt{m_{x,\nu}} \sqrt{2w(1 + \alpha_{\nu}w)}}.$$

Conservation-law form

$$\frac{\partial \Phi_{\nu,p}}{\partial t} + \frac{\partial}{\partial x} [a_{\nu}^1 \Phi_{\nu,p}] + \frac{\partial}{\partial w} [a_{\nu,p}^2 \Phi_{\nu,p}] + \frac{\partial}{\partial \phi} [a_{\nu,p}^3 \Phi_{\nu,p}] = \mathcal{Q}_{\nu,p}[\Phi]s(w)$$

Runge-Kutta time integration

We use a Runge-Kutta time discretization.

Runge-Kutta

We advance in time by the third order Total Variation Diminishing Runge-Kutta scheme: if the evolution equation reads

$$H_{\nu,p}(\Phi) := -\frac{\partial}{\partial x} [a_{\nu,p}^1 \Phi_{\nu,p}] - \frac{\partial}{\partial w} [a_{\nu,p}^2 \Phi_{\nu,p}] - \frac{\partial}{\partial \phi} [a_{\nu,p}^3 \Phi_{\nu,p}] + \mathcal{Q}_{\nu,p}[\Phi]s(w)$$

(no explicit time-dependency), then

- 1 $\Phi_{\nu,p}^{(1)} = \Delta t H_{\nu,p}(\Phi^n)$
- 2 $\Phi_{\nu,p}^{(2)} = \frac{3}{4} \Phi_{\nu,p}^n + \frac{1}{4} \Phi_{\nu,p}^{(1)} + \frac{1}{4} \Delta t H_{\nu,p}(\Phi^{(1)})$
- 3 $\Phi^{n+1} = \frac{1}{3} \Phi_{\nu,p}^n + \frac{2}{3} \Phi_{\nu,p}^{(2)} + \frac{2}{3} H_{\nu,p}(\Phi^{(2)})$

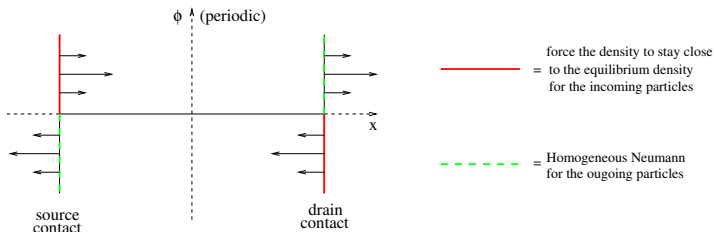
Boundary conditions for the BTE

x-derivative

We use inflow/outflow b.c.: for the incoming particles

$$f_{\nu,p}(t, -x, w, \phi) = \frac{\varrho_{\nu,p}^{\text{eq}}(0)}{\varrho_{\nu,p}(0)} f_{\nu,p}(t, 0, w, \phi),$$

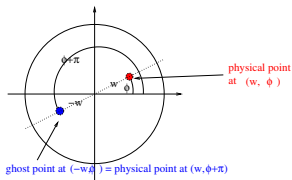
so as to try having $\int_{\mathbb{R}^2} f_{\nu,p}(t, 0, \mathbf{k}) d\mathbf{k} = \varrho_{\nu,p}^{\text{eq}}$. For the outgoing particles, we just use homogeneous Neumann b.c.



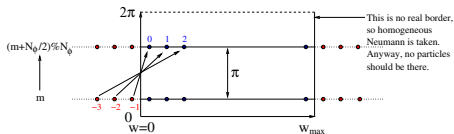
Boundary conditions for the BTE

w-derivative

$w = 0$ is no real boundary; ghost points at $(-w, \phi)$ are physical points at $(w, \phi + \pi)$.
 At $w = w_{max}$ there should be no particles, for properly chosen meshes: just use homogeneous Neumann b.c.



WAVE VECTOR VIEW



Ghost points for negative energy are physical points for a π -shifted angle.

(ENERGY, ANGLE)-VIEW

Integrating the scattering operator

Elastic phenomena

$$Q_{\nu,p}[\Phi]s_{\nu}(w) = C_1^Q \sum_{p'} \frac{1}{W_{(\nu,p') \leftrightarrow (\nu,p)}} \mathbb{I}_{\{\Gamma_0 \geq 0\}} \\ \times \left[s_{\nu}(w) \int_{\phi'=0}^{2\pi} \Phi_{\nu,p'}(\Gamma_0, \phi') d\phi' - 2\pi \Phi_{\nu,p} s_{\nu}(\Gamma_0) \right]$$

Energy gap

When electrons change their state from (ν, p) to (ν', p') , energy jumps appear:

$$\Gamma_0(x, w) = \epsilon_{\nu,p}^{\text{tot}}(x, w) - \epsilon_{\nu',p'}(x).$$

Remark, nevertheless, that they do not exchange energies with the phonons (elastic interaction).

Integrating the scattering operator

Here go the formulae for the integration of the collisional operator in the ellipsoidal dimensionless variables.

Inelastic phenomena

$$\begin{aligned}
 & \mathcal{Q}_{\nu,p}[\Phi]s_{\nu}(w) \\
 &= C^{\mathcal{Q}}s_{\nu}(w) \sum_{\nu',p'} \frac{\gamma_{\nu' \rightarrow \nu} N_{\nu' \rightarrow \nu}}{W_{(\nu',p') \leftrightarrow (\nu,p)}} \mathbb{I}_{\{\Gamma_- \geq 0\}} \int_{\phi'=0}^{2\pi} \Phi_{\nu',p'}(\Gamma_-, \phi') d\phi' \\
 &+ C^{\mathcal{Q}}s_{\nu}(w) \sum_{\nu',p'} \frac{\gamma_{\nu' \rightarrow \nu} (N_{\nu' \rightarrow \nu} + 1)}{W_{(\nu',p') \leftrightarrow (\nu,p)}} \mathbb{I}_{\{\Gamma_+ \geq 0\}} \int_{\phi'=0}^{2\pi} \Phi_{\nu',p'}(\Gamma_+, \phi') d\phi' \\
 &- C^{\mathcal{Q}}2\pi \Phi_{\nu,p}(w, \phi) \sum_{\nu',p'} \frac{\gamma_{\nu \rightarrow \nu'} N_{\nu \rightarrow \nu'}}{W_{(\nu,p) \leftrightarrow (\nu',p')}} \mathbb{I}_{\{\Gamma_+ \geq 0\}} s_{\nu'}(\Gamma_+) \\
 &- C^{\mathcal{Q}}2\pi \Phi_{\nu,p}(w, \phi) \sum_{\nu',p'} \frac{\gamma_{\nu \rightarrow \nu'} (N_{\nu \rightarrow \nu'} + 1)}{W_{(\nu,p) \leftrightarrow (\nu',p')}} \mathbb{I}_{\{\Gamma_- \geq 0\}} s_{\nu'}(\Gamma_-)
 \end{aligned}$$

Integrating the scattering operator

Energy gaps

When electrons change their state from (ν, p) to (ν', p') , energy jumps appear:

$$\Gamma_{\pm}(x, w) = \epsilon_{\nu, p}^{\text{tot}}(x, w) - \epsilon_{\nu', p'}(x) \pm \frac{\hbar\omega}{\kappa_{\text{B}}T_{\text{L}}}$$

Remark that, for inelastic interactions, they exchange energies $\hbar\omega$ with the phonons.

Occupation numbers

The occupation numbers read

$$N_{\nu \rightarrow \nu'} = \frac{\sqrt{\frac{m_{x, \nu} m_{y, \nu}}{m_{x, \nu'} m_{y, \nu'}}} \frac{1+2\alpha_{\nu}}{1+2\alpha_{\nu'}} e^{\frac{\hbar\omega}{\kappa_{\text{B}}T_{\text{L}}}} + 1}{\left(e^{\frac{\hbar\omega}{\kappa_{\text{B}}T_{\text{L}}}} + 1 \right) \left(e^{\frac{\hbar\omega}{\kappa_{\text{B}}T_{\text{L}}}} - 1 \right)},$$

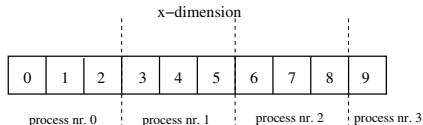
for intra-valley phenomena ($\gamma_{\nu \rightarrow \nu'} = 0$ for $\nu' \neq \nu$), reduce to the well-known

$$N = \frac{1}{e^{\frac{\hbar\omega}{\kappa_{\text{B}}T_{\text{L}}}} - 1}.$$

Outline

- 1 The model
 - Introduction
 - Modelling
- 2 Numerical schemes
 - Iterative schemes for the Schrödinger-Poisson block
 - Solvers for Schrödinger and Poisson
 - Numerical methods for the BTE
 - Parallelization
- 3 Experiments
 - Time-dependent simulations
 - Comparison to Monte-Carlo
 - Plasma oscillations (from the one-valley solver)

Parallelization: 1D block decomposition



The BTE

In order to parallelize Runge-Kutta, we cut the x -dimension:

$$H_{\nu,p}(\Phi) = -\frac{\partial}{\partial x} \left[a_{\nu}^1 \Phi_{\nu,p} \right] - \frac{\partial}{\partial w} \left[a_{\nu,p}^2 \Phi_{\nu,p} \right] - \frac{\partial}{\partial \phi} \left[a_{\nu,p}^3 \Phi_{\nu,p} \right] + \mathcal{Q}_{\nu,p}[\Phi]s(w),$$

We need MPI to exchange data among different processes, namely for $\frac{\partial}{\partial x} \left[a_{\nu}^1 \Phi_{\nu,p} \right]$.

The Schrödinger equation

Same decomposition for the eigenvalue problem, in which x only acts as a parameter:

$$-\frac{\hbar^2}{2} \frac{d}{dz} \left[\frac{1}{m_{z,\nu}} \frac{d\psi_{\nu,p}[V]}{dz} \right] - q(V + V_c) \psi_{\nu,p}[V] = \epsilon_{\nu,p}[V] \psi_{\nu,p}[V].$$

Parallelization of Newton-Raphson

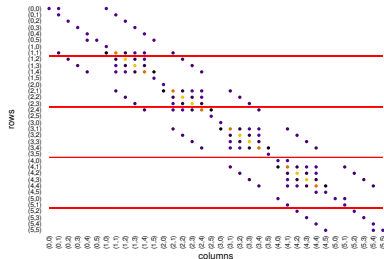


Figure : Decomposition of (x, z) taken as a unique dimension.

Updating the potential

$$-\operatorname{div}(\varepsilon_R \nabla V^{\text{new}}) + \int_0^{L_z} \mathcal{A}(z, \zeta) V^{\text{new}}(\zeta) d\zeta = -\frac{q}{\varepsilon_0} (N - N_D) + \int_0^{L_z} \mathcal{A}(z, \zeta) V^{\text{old}}(\zeta) d\zeta$$

The tasks are shared among the processes: the sole MPI-exchange is V^{new} .

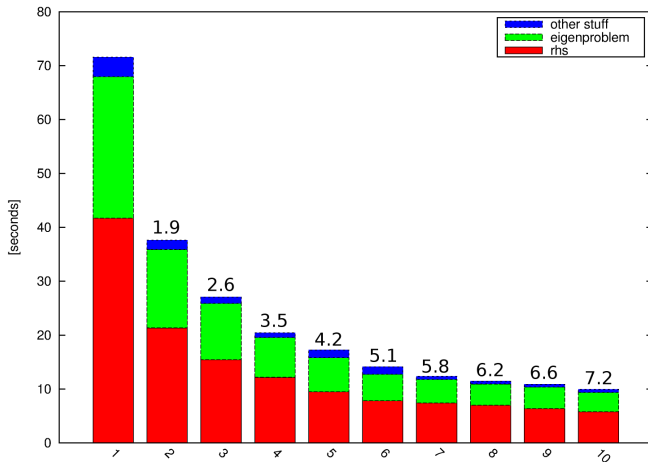
Outline

- 1 The model
 - Introduction
 - Modelling
- 2 Numerical schemes
 - Iterative schemes for the Schrödinger-Poisson block
 - Solvers for Schrödinger and Poisson
 - Numerical methods for the BTE
 - Parallelization
- 3 Experiments
 - **Time-dependent simulations**
 - Comparison to Monte-Carlo
 - Plasma oscillations (from the one-valley solver)

Long-time behavior

We propose now some results relative to the long-time behavior of the system.

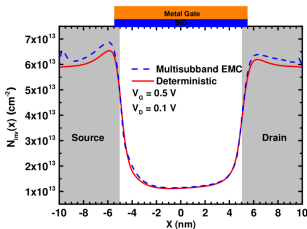
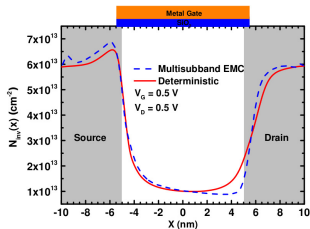
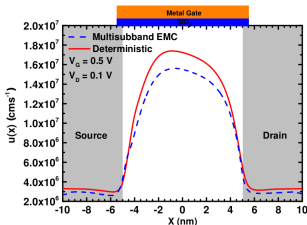
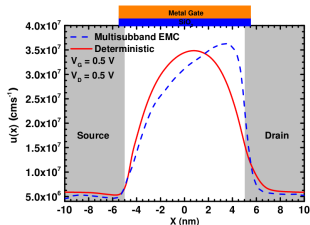
Parallel performances



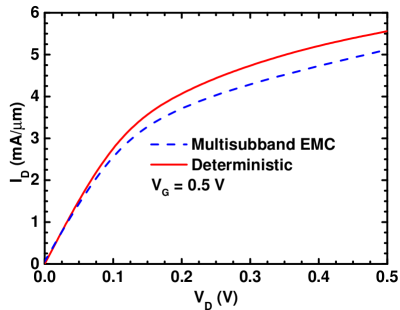
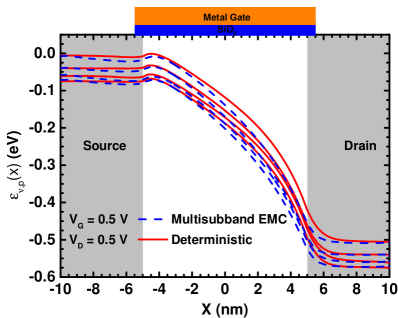
Outline

- 1 The model
 - Introduction
 - Modelling
- 2 Numerical schemes
 - Iterative schemes for the Schrödinger-Poisson block
 - Solvers for Schrödinger and Poisson
 - Numerical methods for the BTE
 - Parallelization
- 3 Experiments
 - Time-dependent simulations
 - **Comparison to Monte-Carlo**
 - Plasma oscillations (from the one-valley solver)

Comparison to Monte-Carlo

(a) For a $V_D = 0.1$ V bias(b) For a $V_D = 0.5$ V bias(c) For a $V_D = 0.1$ V bias(d) For a $V_D = 0.5$ V bias

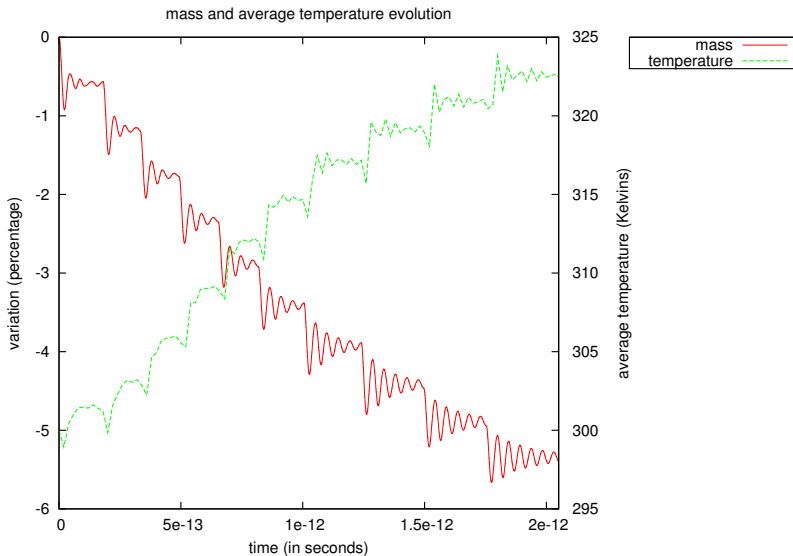
Comparison to Monte-Carlo



Outline

- 1 The model
 - Introduction
 - Modelling
- 2 Numerical schemes
 - Iterative schemes for the Schrödinger-Poisson block
 - Solvers for Schrödinger and Poisson
 - Numerical methods for the BTE
 - Parallelization
- 3 Experiments
 - Time-dependent simulations
 - Comparison to Monte-Carlo
 - Plasma oscillations (from the one-valley solver)

Mass and temperature oscillations



Numerically-computed oscillations

The plasma frequency is given by

$$\omega_p = \sqrt{\frac{q^2 N_e}{\epsilon_R \epsilon_0 m_\star}}$$

N_D^{high} ($\times 10^{26} \text{m}^{-3}$)	ϵ_R	m_\star	N_e ($\times 10^{26} \text{m}^{-3}$)	ω_{num} ($\times 10^{14} \text{s}^{-1}$)	ω_p ($\times 10^{14} \text{s}^{-1}$)	Ratio $\frac{\omega_{\text{num}}}{\omega_{\text{ref}}}$	Expected Ratio
1	11.7	0.5	.400	$\omega_{\text{ref}} = 1.344$	1.475	1	/
2	11.7	0.5	.783	2.051	2.064	1.52	$\sqrt{2}$
4	11.7	0.5	1.544	2.813	2.899	2.09	2
1	5.85	0.5	.400	1.848	2.086	1.37	$\sqrt{2}$

MERCI !